Cell Oncol. (2016) 39:287–293
DOI 10.1007/s13402-016-0279-3

SHORT COMMUNICATION

Inactivation of CYLD in intestinal epithelial cells exacerbates colitis-associated colorectal carcinogenesis - a short report

Demetrios N. Karatzas[1] · Konstantinos Xanthopoulos[1] · Panorea Kotantaki[1] · Athanasios Pseftogas[1] · Konstantinos Teliousis[2] · Eudoxia G. Hatzivassiliou[3] · Dimitris L Kontoyiannis[4] · Theofilos Poutahidis[2] · George Mosialos[1]

Accepted: 13 March 2016 / Published online: 4 April 2016

Abstract
Purpose CYLD is a tumor suppressor that has been linked to the development of various human malignancies, including colon cancer. The tumor-suppressing function of CYLD is associated with its deubiquitinating activity, which maps to the carboxyl-terminal region of the protein. In the present study we evaluated the role of intestinal epithelial CYLD in colitis-associated cancer using a conditional mouse CYLD inactivation model.
Methods In order to evaluate the role of CYLD in intestinal epithelial carcinogenesis, mice (*IEC-Cyld*$^{\Delta 9}$ mice) that carry a mutation that eliminates the deubiquitinating domain of CYLD in intestinal epithelial cells (IEC) were generated by crossing *Villin-Cre* transgenic mice to previously generated mice carrying a loxP-flanked *Cyld* exon 9 (*Cyld*^{flx9} mice).
Results We found that *IEC-Cyld*$^{\Delta 9}$ mice did not present spontaneous intestinal abnormalities up to one year of age. However, upon challenge with a combination of genotoxic (AOM) and pro-inflammatory (DSS) agents we found that the number of adenomas in the *IEC-Cyld*$^{\Delta 9}$ mice was dramatically increased compared to the control mice. Inactivation of CYLD in intestinal epithelial cells did not affect the classical nuclear factor-kappaB (NF-κB) and c-Jun kinase (JNK) activation pathways under physiological conditions, suggesting that these pathways do not predispose CYLD-deficient intestinal epithelia to colorectal cancer development before the onset of genotoxic and/or pro-inflammatory stress.
Conclusions Our findings underscore a critical tumor-suppressing role for functional intestinal epithelial CYLD in colitis-associated carcinogenesis. CYLD expression and its associated pathways in intestinal tumors may be exploited for future prognostic and therapeutic purposes.

Keywords CYLD · NF-κB · JNK · Colon cancer · Tumor suppressor

1 Introduction

The cylindromatosis tumor suppressor gene *Cyld* was first linked to oncogenesis after the identification of mutations that disrupt its coding region in patients with familial Brooke-Spiegler syndrome (BSS) suffering from skin adnexal tumors [1]. Subsequent studies provided compelling evidence for a broader tumor suppressing activity of *Cyld* based on correlations observed between down-regulation of *Cyld* expression and tumorigenesis in various tissues. For example, mutations of *Cyld* or down-regulation of its expression have been associated with the development of multiple myeloma, chronic lymphocytic leukemia, melanoma, hepatocellular carcinoma and colon carcinoma [2–6].

Cyld codes for a 956 amino-acid long polypeptide (CYLD) that possesses deubiquitinating activity in its carboxyl-terminal region (reviewed in [7, 8]). Mutations that disrupt the deubiquitinating domain of CYLD have linked the deubiquitinating activity of CYLD to its tumor suppressing activity in primary human patient samples and in CYLD-

✉ George Mosialos
gmosialo@bio.auth.gr

[1] School of Biology, Aristotle University of Thessaloniki, 54124 Thessaloniki, Macedonia, Greece

[2] Laboratory of Pathology, Faculty of Veterinary Medicine, Aristotle University of Thessaloniki, 54124 Thessaloniki, Macedonia, Greece

[3] Laboratory of Biological Chemistry, Medical School, Aristotle University of Thessaloniki, 54124 Thessaloniki, Macedonia, Greece

[4] Biomedical Sciences Research Centre 'Alexander Fleming', 16672 Vari, Greece

deficient mouse models. The deubiquitinating activity of CYLD has been found to be selective towards K63-linked and linear polyubiquitin chains, which are primarily implicated in the assembly of multi-subunit protein complexes and the regulation of protein signaling activities. By virtue of its ability to modulate poly-ubiquitination of various proteins, CYLD is capable of regulating several signaling pathways critical for cell survival and proliferation, including the nuclear factor-kappaB (NF-κB), c-Jun kinase (JNK), p38, Akt and Wnt pathways. An important aspect of the contribution of CYLD to tissue homeostasis is its ability to modulate programmed cell death by apoptosis and necroptosis. CYLD can affect apoptosis by inhibiting excessive activation of NF-κB or prolonged activation of JNK. In addition, CYLD has been identified as an important mediator of necroptosis, which relies on its ability to deubiquitinate receptor-interacting-kinase (RIPK)1 and to facilitate its phosphorylation along with the phosphorylation of RIPK3 [9]. Even though CYLD is capable of regulating multiple signaling pathways, the predominant CYLD-dependent pathway that underlies a particular pathology may be tissue-specific. For example, genetic approaches have revealed that hyper-activation of NF-κB underlies a defective selection of CYLD-deficient thymocytes [10, 11], whereas sustained activation of JNK has been found to be responsible for an extensive apoptosis that initiates liver fibrosis in mice in which CYLD is inactivated in a hepatocyte-specific manner [12]. Therefore, it is important to assess the role of CYLD in specific cell types in order to understand the systemic pathologies that are associated with its deregulation.

Deregulation of CYLD expression has been associated with several intestinal pathologies, including inflammatory bowel disease and colon cancer. Specifically, down-regulation of CYLD expression has been found to be associated with both Crohn's disease and ulcerative colitis in humans [13, 14]. Furthermore, mice with a constitutive deficiency of *Cyld* have been found to be sensitized to colitis-associated cancer development, i.e., they exhibit a dramatic increase in the incidence and multiplicity of intestinal tumors induced by azoxymethane (AOM) and dextran sodium sulfate (DSS) [15]. Although these studies strongly implicate the down-regulation or inactivation of *Cyld* in colitis-associated cancer, the relative contribution of CYLD-deficient lymphoid, myeloid and/or intestinal epithelial cells (IECs) in the observed phenotype has remained unknown.

In the present study we have generated mice carrying a deubiquitinase-deficient *Cyld* gene in their IECs in order to assess the specific role of CYLD in these cells in the development of intestinal pathologies. Our data support a critical contribution of intestinal epithelial CYLD in the prevention of colitis-associated cancer.

2 Materials and methods

2.1 Mouse models

The experiments involving animals were approved by the Aristotle University of Thessaloniki Faculty of Veterinary Medicine Review Board for compliance to FELASA regulations and licensed by the National Veterinary Administration authorities (License No. 94,354/866). Mice (C57BL/6) were kept in bio-containment facilities in individually ventilated cages, fed with sterilized regular mouse chow and given sterilized water ad libitum. Genotyping of the mice was performed by polymerase chain reaction (PCR) analysis of genomic DNA. The following PCR primers were used to characterize the *Cyld* locus: FWD1: 5 -GATGGCTCTT GTCACCACTT-3′, F6: 5′-CGTGAACAGATGTGA TGAAGGC-3′, R6: 5′-CTACCATCCCTGCTAACCAC-3 . The hybridization positions of the FWD1, F6 and R6 primers are depicted in Fig. 1a. The presence of the *Cre* transgene was assessed by PCR of gemonic DNA using the following primers:

oIMR1084: 5 - GCGGTCTGGCAGTAAAAACTATC-3 , oIMR1085: 5 - GTGAAACAGCATTGCTGTCACTT-3 , oIμR7338: 5 -CTAGGCCACAGAATTGAAAGATCT-3 and oIMR7339: 5 -GTAGGTGGAAATTCTAGCA TCATCC-3 . The oIMR1084 and oIMR1085 primers amplify a 102 bp DNA fragment of the *Cre* transgene, whereas the oIMR7338 and oIμR7339 primers were used concurrently with the *Cre*-specific primers to amplify a 324 bp genomic DNA fragment as internal control.

2.2 AOM/DSS protocol

All experiments were performed on six to eight week-old C57BL/6 mice. On day 0, baseline weights were recorded and each mouse was injected intraperitoneally (IP) with 10 mg/kg of AOM (SIGMA-ALDRICH). On day 7, 1.5 % Dextran Sodium Sulfate (DSS) (molecular weight: 36–50 kDa; MP Biomedicals Inc., Cleveland, OH, USA) solution was supplied to the mice ad libitum in the drinking water. On day 14, cages were switched back to standard drinking water for one week. On day 21, the previous DSS cycle was repeated, followed by a 3 month period of regular drinking water supply. After this, the mice were sacrificed using isoflurane. At necropsy, the colon was removed, cut open, rinsed in normal saline and photographed for the counting of grossly visible polyps.

2.3 Antibodies

For immunohistochemistry (IHC) the following primary antibodies were used: (i) rabbit polyclonal antibodies directed

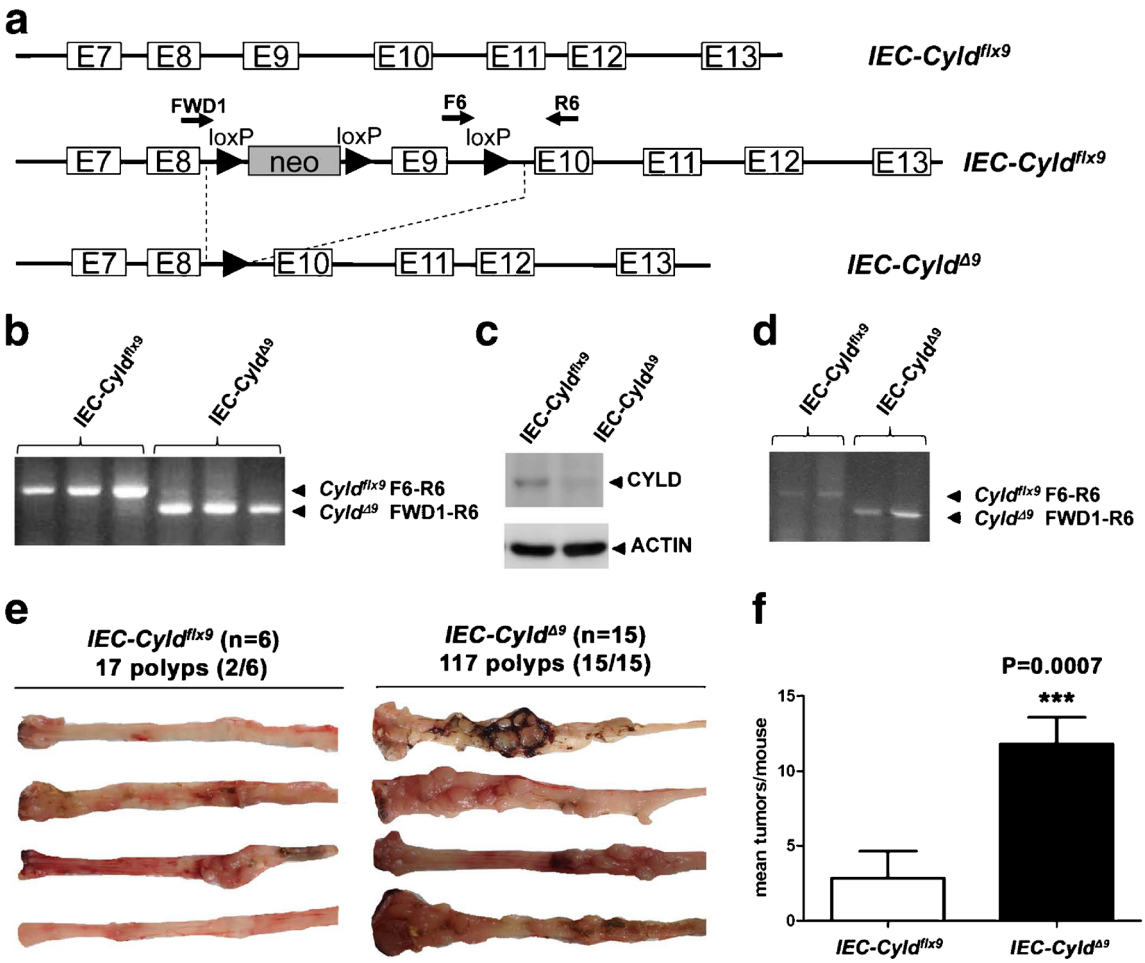

Fig. 1 Conditional inactivation of CYLD in colonic epithelium exacerbates AOM/DSS-induced polypoidogenesis **a** Schematic representation of exons 7–13 (E7-E13) of the murine *Cyld* locus (*Cyld*$^{+}$). The structures of the floxed *Cyld* locus in the absence (*Cyld*^{flx9}) and presence (*Cyld*$^{\Delta 9}$) of the Cre recombinase are shown. The loxP sites are shown as solid triangles. The positions of primers FWD1, F6 and R6 are marked by arrows. **b** PCR analysis of genomic DNA from the intestinal epithelium of *IEC-Cyld*^{flx9} and *IEC-Cyld*$^{\Delta 9}$ mice using a mixture of the FWD1, F6 and R6 primers. The specific PCR product of the floxed *Cyld* locus and the F6-R6 primer pair (*Cyld*^{flx9} F6-R6), as well as the PCR product of the recombined *Cyld* locus and the FWD1-R6 primer pair (*Cyld*$^{\Delta 9}$ FWD1-R6) are indicated by arrowheads. Representative results from three animals per group are shown. **c** Western blot analysis of lysates from IECs, isolated from *Cyld*^{flx9} and *Cyld*$^{\Delta 9}$ mice using anti-CYLD and anti-actin antibodies. The positions of full-length CYLD and actin are marked by arrowheads. **d** PCR analysis of genomic DNA from adenomatous polyps of AOM/DSS-treated *IEC-Cyld*^{flx9} and *IEC-Cyld*$^{\Delta 9}$ mice using a mixture of the FWD1, F6 and R6 primers was performed as described in b. Samples from two animals per group were analyzed and shown. **e** Representative macroscopic appearances of the descending colon and rectum of selected AOM/DSS-treated mice (shown are 4 animals per group). Colonic polyps with typical gross pathologic features are numerous in the colon and rectum of mice lacking functional colonic epithelial cell CYLD, but only a few of them are observed in wild-type treatment-matched controls. **f** CYLD inactivation affects both the multiplicity and occurrence of adenomatous polyps at statistically significant levels. Average numbers of polyps per mouse ± SEM are shown. ***$p < 0.001$

against β-catenin (ThermoFisher Scientific/Lab Vision, Fremont, CA, USA), cleaved caspase-3 and Phospho-JNK (Cell Signaling, Beverly, MA, USA), B-cell lymphoma-3 (Bcl-3, Santa Cruz Biotechnology Inc., Santa Cruz, CA, USA) and (ii) rabbit monoclonal antibodies directed against p65/RelA, c-jun (Cell Signaling, Beverly, MA, USA), cyclin-D1 and Ki-67 (Abcam, Cambridge, UK).

For Western blot analysis anti-CYLD (E-4; Santa Cruz Biotechnology Inc., Santa Cruz, CA, USA) and anti-β-actin (C-4; Santa Cruz Biotechnology Inc., Santa Cruz, CA, USA) antibodies were used.

2.4 Histological analyses

For histologic evaluation, formalin-fixed colon samples were embedded in paraffin, cut at 5 μm, and stained with hematoxylin and eosin (HE) or processed for IHC. Heat-induced antigen retrieval was performed with EDTA buffer, pH 8 for ki-67 or with citrate buffer, pH 6, for the other IHC stains. Rabbit primary antibody binding was detected using a goat anti-rabbit polymer HRP (ZytoChem Plus, Berlin, Germany), after which color was generated using a DAB substrate-chromogen system (ThermoFisher Scientific/Lab Vision, Fremont, CA,

USA). The tissues were counterstained with hematoxylin. Adenomatous polyp counts were compared between groups using Mann-Whitney U analysis. Statistical significance was set at $p < 0.05$. All analyses were performed using the Graphpad Prism version 5.0 for windows (GraphPad Software, San Diego, CA, USA).

3 Results and discussion

Previously, we reported the generation of mice with loxP sites flanking exon 9 of the *Cyld* gene (*Cyld*^{flx9} mice, [16]). Cre-mediated deletion of exon 9 results in a carboxyl terminal truncation of CYLD, which eliminates its deubiquitinating domain. An amino-terminal CYLD polypeptide of 30kD can be expressed upon deletion of exon 9 [16]. In order to evaluate the functional role of CYLD in the intestinal epithelium, we generated mice carrying a deletion of *Cyld* exon 9 specifically in IECs (*IEC-Cyld*$^{\Delta 9}$ mice). This was achieved by crossing *Cyld*^{flx9} mice with *Villin-Cre* mice, which express the Cre recombinase in the intestinal epithelium. By doing so, we found that the *Villin-Cre-Cyld*$^{flx9/flx9}$ (from now on denoted as *IEC-Cyld*$^{\Delta 9}$) mice resulting from these crosses showed efficient deletion of *Cyld* exon 9 and a dramatic reduction in the expression of full-length CYLD in IECs (Fig. 1b-d).

In order to evaluate the role of CYLD in intestinal tumorigenesis, the well-established AOM/DSS protocol was used to determine the susceptibility of mice with intestinal epithelial *Cyld* deficiency to colitis-associated cancer. A single dose of AOM was administered by intraperitoneal injection, followed by two cycles of DSS as described in the materials and methods section. At necropsy, 3 months after the AOM/DSS treatment, typical exophytic polypoid adenomas were found in the colon of the mice. In both *IEC-Cyld*$^{\Delta 9}$ and wild-type control mice adenomatous polyps were located in the descending colon and the rectum (Fig. 1e). All of the *IEC-Cyld*$^{\Delta 9}$ mice (15/15) developed colonic adenomatous polyps. The total number of adenomatous polyps counted was 117 and their sizes ranged from 1 to 7 mm in diameter. By contrast, only 2 out of the 6 control mice developed in total 17 adenomatous polyps, with sizes ranging from 1 to 4 mm in diameter. Genotyping of selected polyps from control and *IEC-Cyld*$^{\Delta 9}$ mice revealed the presence of the expected alleles in each case (Fig.1d). In conclusion, *IEC-Cyld*$^{\Delta 9}$ mice developed somewhat larger and significantly more ($p < 0.001$) adenomatous polyps (mean 11.8 polyps/mouse) than the control mice (mean 2.8 polyps/mouse) (Fig. 1f). The *IEC-Cyld*$^{\Delta 9}$ polyps showed

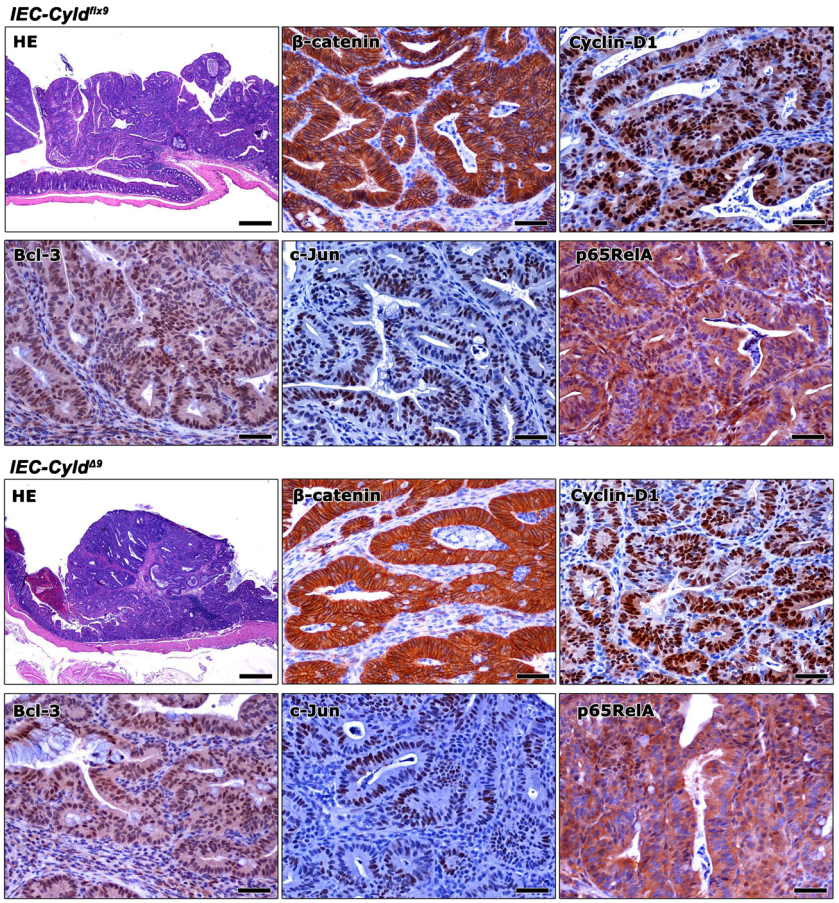

Fig. 2 Histopathological and selected immunohistochemical features of AOM/DSS-induced adenomatous polyps in *IEC-Cyld*$^{\Delta 9}$ and *IEC-Cyld*^{flx9} mice. Microscopic overview of AOM/DSS-induced adenomatous polyps in *IEC-Cyld*$^{\Delta 9}$ and control (*IEC-Cyld*^{flx9}) mice. A typical colonic polyp histopathology with closely-packed tubular glands of abnormal shape and size (tubular adenoma) separated by fibrovascular stroma is observed. Neoplastic gland epithelia universally show abnormal cytoplasmic stabilization of β-catenin and increased cytoplasmic Bcl-3 and p65/RelA expression. Small numbers of neoplastic cells exhibit nuclear β-catenin. Overall, nuclear Bcl-3 and p65/RelA is seen, and high numbers of neoplastic cells show positive immunoreactivity for nuclear cyclin-D1 and c-Jun HE: hematoxylin and Eosin. IHC; Diaminobenzidine chromogen, Hematoxylin counterstain. Scale bars: 250 μm (HE); 50 μm (β-catenin, cyclin-D1, Bcl-3, c-Jun and p65/RelA)

histopathologies typical of mouse colonic polypoid adenomas (Fig. 2) and did not differ from the polyps seen in control mice and other AOM/DSS mouse models described before [17]. In addition, we found by IHC analyses that both *IEC-Cyld*$^{\Delta 9}$ and control mouse polyps shared characteristics of β-catenin stabilization and elevated expression of cyclin-D1, Bcl-3, c-Jun and p65/RelA (Fig. 2). Early invasive adenocarcinoma lesions were not evident in the adenomatous polyps of either experimental groups. The non-polypoid remaining colonic mucosa in both groups of mice was by large normal without signs of chronic residual colitis. These results indicate that the absence of functional CYLD in colonic epithelial cells exacerbates colitis-associated carcinogenesis.

In order to determine whether CYLD inactivation in IECs affects epithelial homeostasis spontaneously, the colons of untreated one-year-old *IEC-Cyld*$^{\Delta 9}$ mice and control mice were examined histologically and, in addition, immunohistochemically for Bcl-3, cyclin-D1, β-catenin, p65/RelA and phosphorylated JNK expression. Both groups of mice exhibited normal colonic histologies. Although we cannot exclude small quantitative differences that cannot be assessed by IHC, *IEC-Cyld*$^{\Delta 9}$ and control IECs exhibited comparable immunohistochemical features of the markers examined, including absence of phospho-JNK and a primarily cytoplasmic localization of p65/RelA (Fig. 3). These findings suggest that the lack of functional CYLD in intestinal epithelia cells does not affect the homeostasis of the intestinal epithelium under physiological conditions.

The signaling pathways that mediate the tumor suppressing role of CYLD in IECs are as yet unknown. One possibility is that lack of functional CYLD causes accelerated proliferation of IECs after injury, which may predispose them to malignant transformation. Alternatively, CYLD inactivation may contribute to programmed cell death resistance. It is known that CYLD can play a positive role in the induction of apoptosis and necroptosis. In case of apoptosis, CYLD may play such a role by inhibiting NF-κB activation by pro-inflammatory cytokines [8, 18]. On the other hand, it has been found that CYLD may facilitate the formation of TNFα-induced necrosomes by deubiquitinating RIP1 and by promoting its interaction with RIP3 and their subsequent phosphorylation [19]. A previous study has revealed a critical role of CYLD in intestinal necroptosis induced by FADD deficiency [20]. Our current results raise the intriguing possibility of an impaired response to AOM-induced genotoxic stress by CYLD-deficient IECs. It has been shown by others that CYLD can facilitate genotoxin-induced apoptosis by reversing the linear ubiquitination of NEMO and limiting the activation of anti-

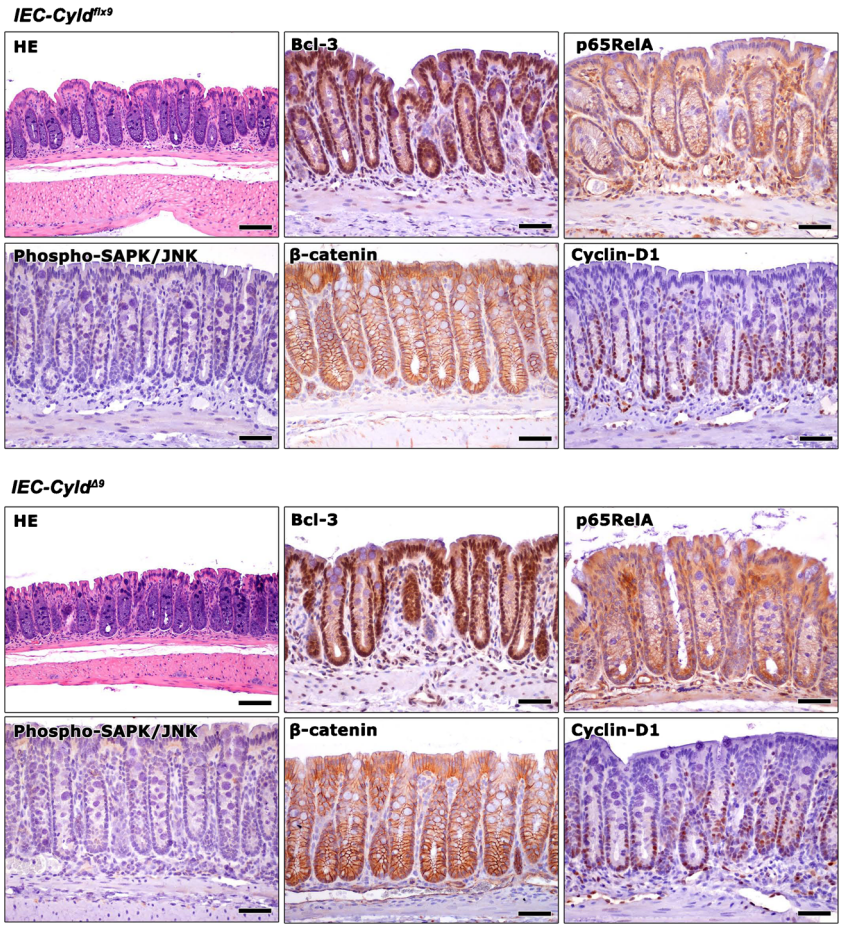

Fig. 3 Conditional inactivation of CYLD does not affect colonic epithelium under normal conditions. One year old untreated *IEC-Cyld*^{flx9} and *IEC-Cyld*$^{\Delta 9}$ mice show a normal colon histology. As expected, the expression of Bcl-3 is constitutive and remains unaffected upon inactivation of CYLD. Likewise, the colon of both groups show baseline cytoplasmic expression of p65/RelA in colonic epithelial and stromal cells, undetectable phosphorylated JNK (phospho-SAPK/JNK) and the expected patterns of β-catenin and cyclin-D1 staining. HE: hematoxylin and eosin. IHC: diaminobenzidine chromogen, hematoxylin counterstain. Scale bars: 100 μm (HE); 50 μm (Bcl-3, p65RelA, phospho-SAPK/JNK, β-catenin and Cyclin-D1)

apoptotic NF-κB-dependent gene expression [21]. Furthermore, it was found that inactivation of CYLD may confer resistance to cancer cells against genotoxic agents [22, 23]. Therefore, it is conceivable that the lack of functional CYLD in IECs may allow the accumulation of AOM-induced mutations by preventing the death of cells that would normally be eliminated due to excessive DNA damage that cannot be repaired properly. As yet, the delineation of the exact mechanism underlying the disturbed homeostasis of CYLD-deficient IECs upon injury requires extended analyses of larger numbers of experimental animals.

CYLD is a well-known negative regulator of the NF-κB and JNK pathways in various cell types. Aberrant activation of either pathway in IECs has been associated with sensitization to colitis-associated polypoidogenesis (reviewed in [24]). Hyper-activation of NF-κB in IECs promotes the expression of cytokines and chemokines leading to an enhanced recruitment of inflammatory cells and a concomitant exacerbation of the inflammatory response. On the other hand, prolonged activation of JNK can lead to enhanced apoptosis and compensatory proliferation that will favor the selection and outgrowth of IECs with improved growth and survival characteristics. However, our analyses did not reveal enhanced nuclear localization of p65/RelA or Bcl3 in CYLD-deficient IECs under physiological conditions, as has been reported by others in other cell types and tissues [12, 25]. These findings argue against a major role of CYLD in maintaining the basal activities of NF-κB and JNK in IECs. Nevertheless, one cannot rule out a role for CYLD in the regulation of a subset of NF-κB- or JNK-dependent genes or the deregulation of these pathways in CYLD-deficient IECs upon certain stress conditions. Another signaling pathway that has been reported to be regulated by CYLD and is relevant to the observed phenotype is the Wnt pathway [26]. More specifically, CYLD can inhibit the Wnt pathway at least in part by deubiquitinating Dishevelled. This observation is of particular interest for the present study, since a hyperactive Wnt pathway is a known contributor to intestinal tumorigenesis [27]. Although we cannot exclude a contribution of certain components of the Wnt pathway, our analysis of β-catenin expression failed to reveal a dramatic deviation in its expression or localization in CYLD-deficient intestinal epithelial cells. Finally, it should be noted that the *Cyld* mutation that was introduced in IECs eliminates the entire deubiquitinating domain of CYLD. Although loss of the deubiquitinating function is likely to be the major cause of the observed phenotype, the elimination of other properties of CYLD such as scaffolding or regulatory protein interactions may very well contribute to the observed phenotype as well. Further elucidation of the specific molecular pathways that mediate the tumor suppressing role of intestinal epithelial CYLD in colitis-associated cancer will be the subject of future studies.

Acknowledgments This work was supported by intramural funding of the School of Biology of Aristotle University of Thessaloniki and by a scholarship of the Hellenic State Scholarships Foundation (to DNK). The authors gratefully acknowledge the support of the Bodossaki Foundation for the acquisition of laboratory equipment that was used for the imaging and the animal husbandry in the present study.

Compliance with ethical standards

Conflict of interest The authors declare no conflict of interest.

References

1. G. R. Bignell, W. Warren, S. Seal, M. Takahashi, E. Rapley, R. Barfoot, H. Green, C. Brown, P. J. Biggs, S. R. Lakhani, C. Jones, J. Hansen, E. Blair, B. Hofmann, R. Siebert, G. Turner, D. G. Evans, C. Schrander-Stumpel, F. A. Beemer, A. van Den Ouweland, D. Halley, B. Delpech, M. G. Cleveland, I. Leigh, J. Leisti, S. Rasmussen, Identification of the familial cylindromatosis tumour-suppressor gene. Nat. Genet. **25**, 160–165 (2000)
2. J. J. Keats, R. Fonseca, M. Chesi, R. Schop, A. Baker, W. J. Chng, S. Van Wier, R. Tiedemann, C. X. Shi, M. Sebag, E. Braggio, T. Henry, Y. X. Zhu, H. Fogle, T. Price-Troska, G. Ahmann, C. Mancini, L. A. Brents, S. Kumar, P. Greipp, A. Dispenzieri, B. Bryant, G. Mulligan, L. Bruhn, M. Barrett, R. Valdez, J. Trent, A. K. Stewart, J. Carpten, P. L. Bergsagel, Promiscuous mutations activate the noncanonical NF-kappaB pathway in multiple myeloma. Cancer Cell **12**, 131–144 (2007)
3. C. M. Annunziata, R. E. Davis, Y. Demchenko, W. Bellamy, A. Gabrea, F. Zhan, G. Lenz, I. Hanamura, G. Wright, W. Xiao, S. Dave, E. M. Hurt, B. Tan, H. Zhao, O. Stephens, M. Santra, D. R. Williams, L. Dang, B. Barlogie, J. D. Shaughnessy Jr., W. M. Kuehl, L. M. Staudt, Frequent engagement of the classical and alternative NF-kappaB pathways by diverse genetic abnormalities in multiple myeloma. Cancer Cell **12**, 115–130 (2007)
4. W. Wu, H. Zhu, Y. Fu, W. Shen, J. Xu, K. Miao, M. Hong, W. Xu, P. Liu, J. Li, Clinical significance of down-regulated cylindromatosis gene in chronic lymphocytic leukemia. Leuk. Lymphoma **55**, 588–594 (2014)
5. R. Massoumi, S. Kuphal, C. Hellerbrand, B. Haas, P. Wild, T. Spruss, A. Pfeifer, R. Fassler, A. K. Bosserhoff, Down-regulation of CYLD expression by snail promotes tumor progression in malignant melanoma. J. Exp. Med. **206**, 221–232 (2009)
6. C. Hellerbrand, E. Bumes, F. Bataille, W. Dietmaier, R. Massoumi, A. K. Bosserhoff, Reduced expression of CYLD in human colon and hepatocellular carcinomas. Carcinogenesis **28**, 21–27 (2007)
7. R. Massoumi, Ubiquitin chain cleavage: CYLD at work. Trends Biochem. Sci. **35**, 392–399 (2010)
8. S. C. Sun, CYLD: a tumor suppressor deubiquitinase regulating NF-kappaB activation and diverse biological processes. Cell Death Differ. **17**, 25–34 (2010)
9. D. M. Moquin, T. McQuade, F. K. Chan, CYLD deubiquitinates RIP1 in the TNFalpha-induced necrosome to facilitate kinase activation and programmed necrosis. PLoS One **8**, e76841 (2013)
10. A. Tsagaratou, E. Trompouki, S. Grammenoudi, D. L. Kontoyiannis, G. Mosialos, Thymocyte-specific truncation of the deubiquitinating domain of CYLD impairs positive selection in a NF-kappaB essential modulator-dependent manner. J. Immunol. **185**, 2032–2043 (2010)
11. A. Tsagaratou, S. Grammenoudi, G. Mosialos, Differential requirement of IKKbeta for CYLD-dependent representation of thymic

and peripheral T cell populations. Eur. J. Immunol. **41**, 3054–3062 (2011)
12. K. Nikolaou, A. Tsagaratou, C. Eftychi, G. Kollias, G. Mosialos, I. Talianidis, Inactivation of the deubiquitinase CYLD in hepatocytes causes apoptosis, inflammation, fibrosis, and Cancer. Cancer Cell **21**, 738–750 (2012)
13. I. Cleynen, E. Vazeille, M. Artieda, H. W. Verspaget, M. Szczypiorska, M. A. Bringer, P. L. Lakatos, F. Seibold, K. Parnell, R. K. Weersma, J. M. Mahachie John, R. Morgan-Walsh, D. Staelens, I. Arijs, G. De Hertogh, S. Muller, A. Tordai, D. W. Hommes, T. Ahmad, C. Wijmenga, S. Pender, P. Rutgeerts, K. Van Steen, D. Lottaz, S. Vermeire, A. Darfeuille-Michaud, Genetic and microbial factors modulating the ubiquitin proteasome system in inflammatory bowel disease. Gut **63**, 1265–1274 (2014)
14. C. M. Costello, N. Mah, R. Hasler, P. Rosenstiel, G. H. Waetzig, A. Hahn, T. Lu, Y. Gurbuz, S. Nikolaus, M. Albrecht, J. Hampe, R. Lucius, G. Kloppel, H. Eickhoff, H. Lehrach, T. Lengauer, S. Schreiber, Dissection of the inflammatory bowel disease transcriptome using genome-wide cDNA microarrays. PLoS Med. **2**, e199 (2005)
15. J. Zhang, B. Stirling, S. T. Temmerman, C. A. Ma, I. J. Fuss, J. M. Derry, A. Jain, Impaired regulation of NF-kappaB and increased susceptibility to colitis-associated tumorigenesis in CYLD-deficient mice. J. Clin. Invest. **116**, 3042–3049 (2006)
16. E. Trompouki, A. Tsagaratou, S. K. Kosmidis, P. Dolle, J. Qian, D. L. Kontoyiannis, W. V. Cardoso, G. Mosialos, Truncation of the catalytic domain of the cylindromatosis tumor suppressor impairs lung maturation. Neoplasia **11**, 469–476 (2009)
17. E. Karamanavi, K. Angelopoulou, S. Lavrentiadou, A. Tsingotjidou, Z. Abas, I. Taitzoglou, I. Vlemmas, S.E. Erdman and T. Poutahidis. Urokinase-type plasminogen activator deficiency promotes neoplasmatogenesis in the colon of mice. Transl. Oncol. **7**, 174–187 e175 (2014)
18. K. Vazquez-Santillan, J. Melendez-Zajgla, L. Jimenez-Hernandez, G. Martinez-Ruiz, V. Maldonado, NF-kappaB signaling in cancer stem cells: a promising therapeutic target? Cell. Oncol. **38**, 327–339 (2015)
19. W. Zhou, J. Yuan, Necroptosis in health and diseases. Semin. Cell Dev. Biol. **35**, 14–23 (2014)
20. P. S. Welz, A. Wullaert, K. Vlantis, V. Kondylis, V. Fernandez-Majada, M. Ermolaeva, P. Kirsch, A. Sterner-Kock, G. van Loo, M. Pasparakis, FADD prevents RIP3-mediated epithelial cell necrosis and chronic intestinal inflammation. Nature **477**, 330–334 (2011)
21. J. Niu, Y. Shi, K. Iwai, Z. H. Wu, LUBAC regulates NF-kappaB activation upon genotoxic stress by promoting linear ubiquitination of NEMO. Embo J **30**, 3741–3753 (2011)
22. W.L. Yang, G. Jin, C.F. Li, Y.S. Jeong, A. Moten, D. Xu, Z. Feng, W. Chen, Z. Cai, B. Darnay, W. Gu and H.K. Lin. Cycles of ubiquitination and deubiquitination critically regulate growth factor-mediated activation of Akt signaling. Sci. Signal. **6**, ra3 (2013)
23. D. Takiuchi, H. Eguchi, H. Nagano, Y. Iwagami, Y. Tomimaru, H. Wada, K. Kawamoto, S. Kobayashi, S. Marubashi, M. Tanemura, M. Mori, Y. Doki, Involvement of microRNA-181b in the gemcitabine resistance of pancreatic cancer cells. Pancreatology **13**, 517–523 (2013)
24. J. Terzic, S. Grivennikov, E. Karin and M. Karin. Inflammation and colon cancer. Gastroenterology **138**, 2101–2114 e2105 (2010)
25. R. Massoumi, K. Chmielarska, K. Hennecke, A. Pfeifer, R. Fassler, Cyld inhibits tumor cell proliferation by blocking bcl-3-dependent NF-kappaB signaling. Cell **125**, 665–677 (2006)
26. D. V. Tauriello, A. Haegebarth, I. Kuper, M. J. Edelmann, M. Henraat, M. R. Canninga-van Dijk, B. M. Kessler, H. Clevers, M. M. Maurice, Loss of the tumor suppressor CYLD enhances wnt/beta-catenin signaling through K63-linked ubiquitination of dvl. Mol. Cell **37**, 607–619 (2010)
27. B. Sumithra, U. Saxena, A. B. Das, Alternative splicing within the wnt signaling pathway: role in cancer development. Cell. Oncol. **39**, 1–13 (2016)